Comparison between electromagnetic and thermal stress induced by Direct Current flow in IGBT bond wires

Hassen Medjahed, Paul-Etienne Vidal, Bertrand Nogarède

Comparison between electromagnetic and thermal stress induced by Direct Current flow in IGBT bond wires

H. MEDJAHED[a (Ph-D student)], P.-E. VIDAL[a (Ph-D)], B. NOGAREDE[b (Prof.)]

[a] Université de Toulouse, INP Toulouse, LGP, 47 avenue d'Azereix 65016 TARBES Cedex, France. Corresponding author : paul-etienne.vidal@enit.fr
[b] Université de Toulouse, INP Toulouse, LAPLACE – CNRS UMR 5213, 2, rue Charles Camichel BP 7122, 31071 Toulouse Cedex 7, France.

Summary

This study is focused on the IGBT wire bond behaviour. We apply a direct current flow within the wire to reproduce the thermal cycling test used in reliability studies. On one hand we compare the temperature distribution between 3D FEM simulation and the experimental temperature measurement. We also point out the Von-Mises stress obtained. On the other hand we compare the thermo-mechanical results to those obtained with a 1D simplified thermal model. We also take into account the electromagnetic force and the mechanical stress that could be induced on the bond wire. Some experimental and simulation results are given.

1 Introduction and scope of the study

In many applications, one can find some power electronics components. They allow transferring the electrical energy between the electrical source and the electrical machine. Since many years the wish of studies is to obtain a more integrated static converter: that is to say more power into less volume. Then, due to the stress obtained, the power electronic reliability becomes an important field of study [1] [2].

In the field of power inverters, the use of Insulated Gate Bipolar Transistor (IGBT) leads to specific reliability studies. One main contributor to IGBT failure is related to bond wires. Indeed the fatigue is caused either by the shear stresses between the bond pad and the silicon device or by repetitive wire flexure [3] [4].

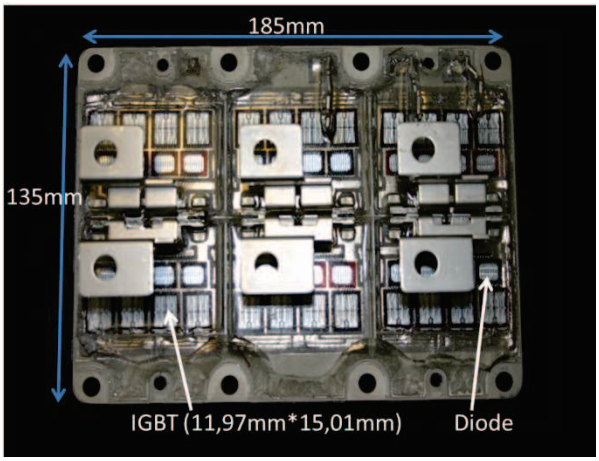

Figure 1 : Example of an open IGBT.

It occurs after electrical, thermal and mechanical phenomenon interactions. The type of IGBT modules used for our application is three-phase 1500A – 3300 V, built with 24 elementary IGBTs and their own associated diodes in parallel. It is illustrated in Figure 1.

Our study reveals the mechanical stresses due to the current flow in steady state. We will compare the Von-Mises stress distribution obtained by active thermal cycling and the distribution induced by electromagnetic force.

2 Experimental and numerical set-up

2.1 The system studied

We design four simple devices based on single or two parallel wires. They are bonded on copper substrate from one side and to an active chip for the other side. Our two first devices are illustrated in Figure 2.

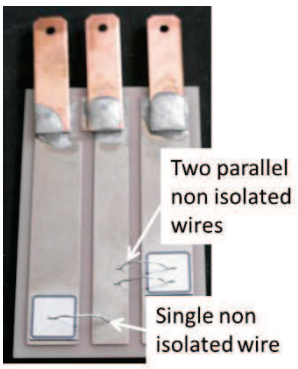

Figure 2 : Simple device design.

But for most of our experiments we also designed two other devices on which the single or the two parallel wires are alone: the substrates are identical but active chips are not used. In fact, the wires are set apart. They are considered as isolated wires or stand alone.

We use the classical material and geometry mainly encountered in high power IGBT modules. Indeed, the wires used are ultrasonic bonded. They are constituted of Al 99,99%. The geometry itself is adapted from the one observed on different IGBT modules.

2.2 DC input

The direct current applied (10 A) is obtained from IGBT specification related to the number of wires. It corresponds to a current density of $50.9*10^6$ A/m^2 flowing within the wire. As we said, it is linked with the datasheet

Properties	*Al*	*Cu*	*AlN*
Thermal conductivity λ (W m^{-1} °K^{-1})	237	401	180
Electrical conductivity $\sigma = \frac{1}{\rho_e}$(S m^{-1})	3.69*10^{+7}	5.96*10^{+7}	10^{-14}
Volume density ρ(kg m^3)	2700	8900	3260
Specific heat C_p (J kg^{-1} °K^{-1})	897	380	740
Young's modulus E (MPa)	6.6*10^4	11*10^4	31*10^4
Poisson 's ratio ν	0.35	0.343	0.24
Coefficient of thermal expansion α (@23)°	2.3*10^{-5}	3*10^{-5}	4.5*10^{-6}

Table 1 : Material properties.

and the analysis of an open module. But it is also correlated with the real current magnitude experienced. For the example given, the maximal recommended current divided by the number of IGBTs and the number of wires is expressed by:

Eq 1 :

$$I = \frac{I_{max}}{N_{IGBT}N_{wires}} = \frac{1500}{24 * 8} = 7{,}8A$$

Nevertheless the maximal current applied (and so experienced) by the module is $1{,}5 * I_{max} = 2250A$. Consequently the value of $10A$ is taken as a mean value experienced by $500\mu m$ diameter bonded wires.

2.3 3D FEM

To solve and obtain the mechanical stress experienced by the wires, we use the ABAQUS software. We first use the electro - thermal resolution, followed by thermal - displacement analysis. For example, we build a FEM based on a single isolated wire, as shown in Figure 3. Parameters used are given in Table 1.

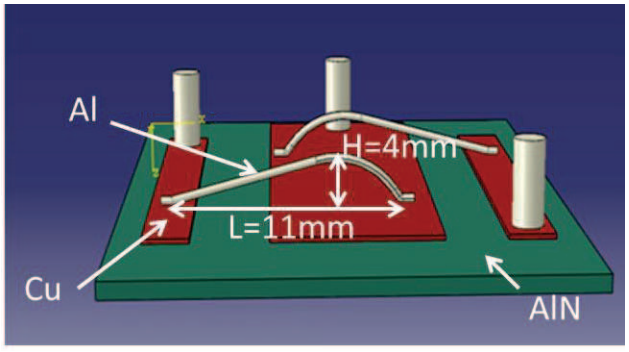

Figure 3 : 3D single and isolated wire numerical model.

2.4 1D simplified thermal model

We think that sometimes the design of high power module will require fast optimization tools. Indeed, we developed a simplified wire thermal model. An analytic 1D thermal model is expressed according simplification hypothesis. It is based on the 3D thermal flow expression:

Eq 2 :

$$\lambda\left(\frac{\partial}{\partial x}\frac{\partial\theta}{\partial x} + \frac{\partial}{\partial y}\frac{\partial\theta}{\partial y} + \frac{\partial}{\partial z}\frac{\partial\theta}{\partial z}\right) + P - \frac{hP_e}{S}(\theta - \theta_a) = \rho C_p \frac{\partial\theta}{\partial t}$$

with θ the temperature at given x, y, z coordinate. θ_a is the environmental temperature. S is the wire cross section, whereas P_e is the wire circumference. Other parameters are given in Table 1. P is the power flow within the wire due to the current density flux such as: $P = \rho_e(\frac{I}{S})^2$. Where ρ_e is the electrical resistance and I the DC magnitude. In steady state and considering that the wire section is not relevant in comparison to the wire length leads to:

Eq 3 :

$$\frac{\partial\theta}{\partial y} = 0 \; and \; \frac{\partial\theta}{\partial z} = 0$$

Thanks to this simplification, we can express the temperature distribution along the wire by:

Eq 4 :

$$\lambda(\frac{d\theta}{dx})^2 + \rho(\frac{I}{S})^2 - \frac{hP_e}{S}(\theta - \theta_a) = 0$$

This is our simplified 1D thermal expression. Then, Eq 4 is expressed as:

Eq 5 :

$$(\frac{d\theta}{dx})^2 - a\theta + b = 0$$

Where a and b are obtained by identification thanks to Eq 4. Finally we find the final solution which expresses the temperature distribution along the wire x coordinate:

Eq 6 :

$$\theta(x) = Ae^{a^{0.5}x} + Be^{-a^{0.5}x} + \frac{b}{a}$$

A, B are obtained thanks to the boundary conditions:

Eq 7 :

$$x = 0 \quad \theta(0) = T_1$$
$$x = L \quad \theta(L) = T_2$$

T_1, T_2 are two temperatures which can be different. They can be given by the user itself (desired substrate temperature for instance) or by specific measurements. Then Eq 6 is sampled and computed in Scilab environment [5].

2.5 Electromagnetic force expression

In order to determine the analytical expression of the electromagnetic force induced, we consider the wire as two segments linked each other by one angle α and flowed by the same current, I, (Figure 4).

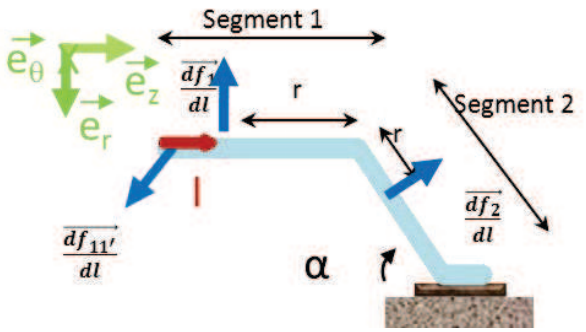

Figure 4 : Scheme of the electromagnetic model.

We applied the Biot-Savart law to determine the magnetic field obtained along the wire. Hereabouts, considering the wire length larger than the cross-sectional diameter, we use the long wire hypothesis. We first consider the elementary magnetic field expression given by a segment (n°1 with a limited length), on point M_2 of the segment n°2 (all vectors are expressed in bold type):

Eq 8 :

$$\boldsymbol{dB_1}(M_2) = \frac{\mu_0}{4\pi} I \frac{\cos(\frac{\pi}{2} - \alpha)}{D} d\alpha \, \boldsymbol{e_\theta}$$

With $D = r\sin(\alpha)$. r is the distance on each segment related to the upper wire loop, α is the angle made between the bond wire and the Si chip. μ_0 is the air magnetic permeability. Then we demonstrated for different DC current values that the most part of the field is concentrated near the upper wire loop. For example, the Figure 5 is given for a DC magnitude ($10\,A$) and a given angle ($\alpha =$ 51.5 °). We can see that beyond the distance of 50 μm the field is not relevant. Consequently the forces will be found near the segment connection points.

We also express the elementary field given by segment n°2, $\boldsymbol{dB_2}$. Finally, the global elementary magnetic field is computed by:

Eq 9 :

$$\boldsymbol{dB} = \boldsymbol{dB_1} + \boldsymbol{dB_2}$$

By integrating Eq 9, we obtained the magnetic field due to the single wire: $\boldsymbol{B}$.

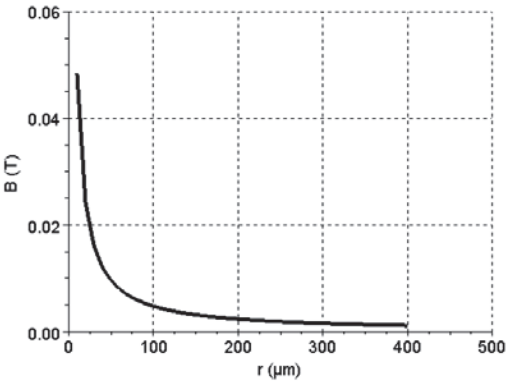

Figure 5 : Magnetic field evolution for a wire segment.

To finish, we apply the Laplace Force to such device:

Eq 10 :

$$\boldsymbol{df} = I\boldsymbol{dl} \times \boldsymbol{B}$$

Based on Eq 10 we determine the elementary force ($\frac{N}{m}$) on each segment. This is what we called the "own wire force" on each segment:

Eq 11 :

$$\frac{\boldsymbol{df_1}}{\boldsymbol{dl}} = \frac{\mu_0}{4\pi r} I^2 \tan(\frac{\alpha}{2}) \left(\sin(\alpha)\boldsymbol{e_z} - \sin(\frac{\pi}{2} - \alpha)\boldsymbol{e_r}\right)$$

$$\frac{\boldsymbol{df_2}}{\boldsymbol{dl}} = \frac{\mu_0}{4\pi r} I^2 \tan(\frac{\alpha}{2}) \, \boldsymbol{e_r}$$

A similar study can be done to evaluate the consequence of having two wires in parallel. Indeed, the Laplace force between the wires could be expressed as:

Eq 12 :

$$\frac{\boldsymbol{df_{11'}}}{\boldsymbol{dl}} = \frac{\mu_0}{4\pi a} I^2 \tan(\frac{\alpha}{2}) \left(\sin(\theta_2) - \sin(\theta_1)\right)\boldsymbol{e_\theta}$$

a is the distance between two parallel wires typically $a = 1mm$, and $\theta_1 = \tan^{-1}(\frac{L-r}{a})$, $\theta_2 = \tan^{-1}(\frac{r}{a})$. L is the wire lenght. Considering the device studied, $L = 12.3\,mm$.

Firstly, computing numerical values leads to consider that the main effect will be produced on a same wire between both segments.

We finally apply the elementary force distribution, Eq 11, Eq 12, on our 3D numerical model.

3 Experimental and numerical results

3.1 Thermal stress induced

Thanks to the numerical model we ran an electro thermal analysis and obtained the temperature distribution along the wire as illustrated in Figure 6, (red curve). It is obtained from 3D mean value computation along the wire path. We applied the DC supply already defined. Afterwards we measured on an experimental test bench, the temperature dispatching along the bond wire, (blue curve). We also reported (black curve) the temperature distribution along the wire using the 1D simplified model described (§2.4 - Eq 6). The accuracy of our numerical (red curve) or analytic (black) models to the measured temperature (blue) is allowed.

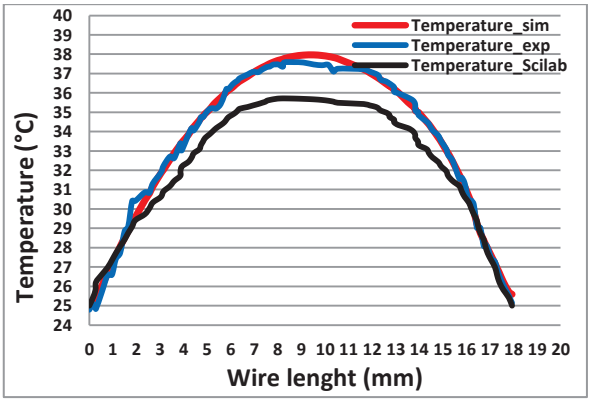

Figure 6 : Temperature dispatching along the wire.

The measurement and the 3D simulation results are similar, whereas the simplified model presents an error. We can point out that the 1D thermal model does not take into account the whole substrate. Moreover, it only considers two single temperature point as boundary conditions: T_1, T_2. They are similar to those defined in Eq 7. In addition, the parameters used are taken constant, and the temperature is also considered constant within the wire cross-sectional area S. But as far as the 3D FEM simulation is concerned, depending of the numbers of elements used and the total simulation time desired, the running time can vary from few minutes to hours. Whereas the simplified model results are computed in few seconds. Consequently we can say that for first and simple studies, the 1D simplified thermal model is meaningful.

3.2 Von-Mises mechanical stress

By this way, we prove the accuracy of our simulation model. Indeed, the temperature dispatching experienced by the wires, leads to maximal principal stress distribution. It is noted that the maximal value (10 MPa) is located at the tail of the wire, just in front of the heel area, as reported in [1], (Figure 7).

We made further works to point out the links between the wire bond angle and the current magnitude. The indicator used is the maximal stress value observed as reported in Table 2.

DC magnitude I	Angle α			
	20°	40°	60°	80°
5 A	2.1	2.9	2.75	3.8
10 A	8.3	11.5	10.9	15.7
15 A	18.8	26	24	NR
	Maximal Von-Mises stress (MPa)			

Table 2 : DC magnitude and angle sweep - maximal Von Mises stress.

NR means non-relevant. It is due to our linear stress – displacement law.

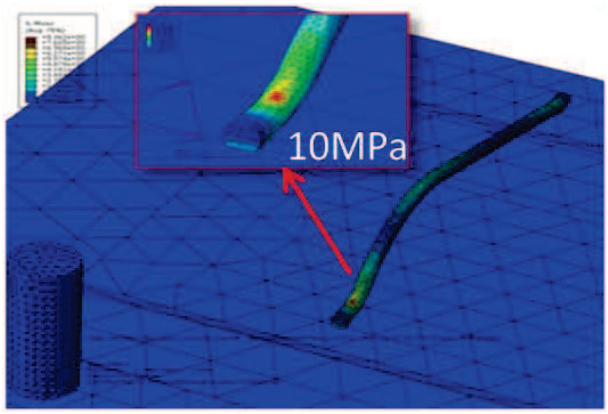

Figure 7 : Electro thermomechanical stress obtained by DC supply.

In a second step we apply the electromagnetic force distribution to 3D FEM. Introducing the expressions obtained in Eq 11 and Eq 12, we computed a force-displacement analysis. Then the results demonstrate that the Von-Mises stress obtained is not relevant compared with the thermo mechanical one.

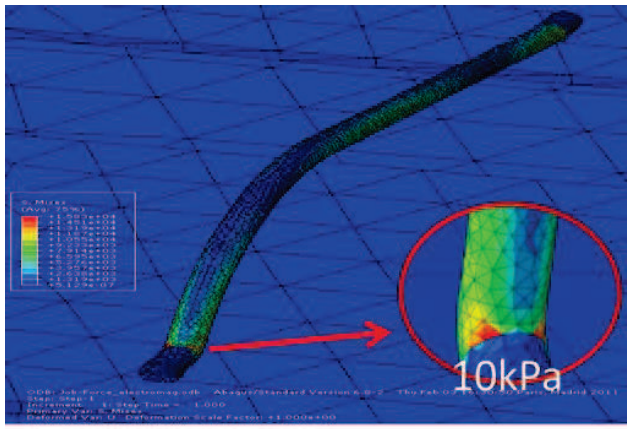

Figure 8 : Von-Mises stress obtained with electromagnetic force.

3.3 Displacement measurement

One stress consequence is the displacement measured along the bond wire itself. The displacement value is checked thanks to Digital Image Stereo-Correlation. We pointed out a 6 μm displacement in the "Z" axis of a Galilean reference frame as presented in Figure 9. Because of

the camera precision we cannot state that the X or Y displacement shown is relevant in such environment (the precision given is $\pm 1 \mu m$).

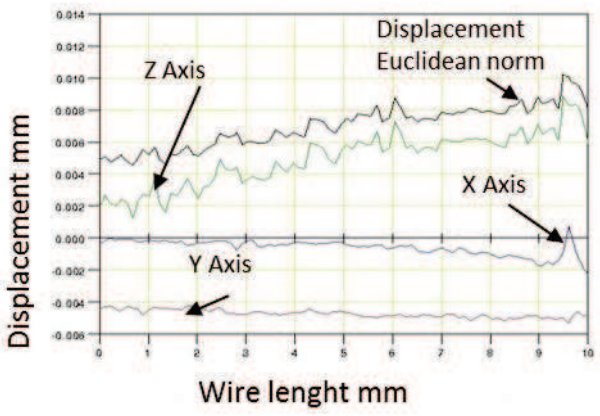

Figure 9 : 3D displacement mesasurements

The displacement Euclidean norm is
$Total_{displacement_{norm}} = \sqrt{x^2 + y^2 + z^2}$.
With x the displacement value in the x-axis, y the displacement value in the y-axis and z the displacement value in the z-axis.
Considering the Z displacement of a single wire, we measured the maximal displacement with different DC magnitude, as given in Table 3.

DC magnitude	Isolated wire Z-displacement	Non isolated wire Z-displacement
5 A	2 µm	4 µm
10 A	6 µm	10 µm
15 A	14 µm	26 µm
20 A	28 µm	Wire fuse
25 A	60 µm	Wire fuse

Table 3 : Maximal Z-displacement with DC magnitude sweep for single wire devices.

It is noted that the measurement with an active chip were not possible when the DC value is upper than $15A$. Effectively the wire fused before the measurement. With $10\ A$, in such environment we pointed out a maximal wire temperature of $200\ °C$ whereas the temperature chip was $168\ °C$. At this moment the displacements encountered reached 150 % of the initial value.
We illustrate such displacements measurements in Figure 10. One can distinguish the Z-displacement values for the whole packaging, for a $10\ A$ current. We automatically extracted from such a figure the curves reported in Figure 9.
We could also check that a part of the left and upper part of the Si device is moving.
With two parallel isolated wires and doing the same experiments leads to Table 4.

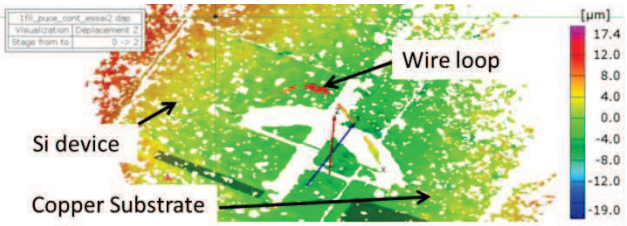

Figure 10 : Postprocessed displacement image –single wire, Si chip connected.

As already said, displacements values lower than $2\ \mu m$ should not be taken into account. Nevertheless, looking at $12.5\ A$ experience, the Z-displacement is equivalent to the one encountered with single wires, whereas X and Y displacements proved the existence of interaction force between wires. It makes us wonder how such displacements can be linked with the expression force pointed out in Eq 11 and Eq 12.

DC magnitude per wire	X-Displacement per wire	Y-Displacement per wire	Z-Displacement per wire
2.5 A	0 µm	1 µm	2 µm
5 A	0.75 µm	1.5 µm	3 µm
7.5 A	1 µm	2 µm	4.5 µm
10 A	3 µm	3.75 µm	7 µm
12.5 A	4.5 µm	6 µm	13 µm

Table 4 : Displacements with two parallel isolated wires.

4 Conclusion

The main objective is to best characterize the maximal principal stress experienced by a bond wire during DC operation mode. The thermal cycle experienced by the bond wire is due to the direct current flowing within the wire. We realized precise thermo-mechanical simulations and compared them to experimental results and analytic models. Thanks to the 3D numerical study we produced the maximal principal stress distribution by using the Von-Mises yield criterion. We also took into account the electromagnetic effects. We finally conclude that they will not be relevant in such current operating mode, as far as the mechanical stress value is concerned. But in the both case, it is noted that the maximal mechanical stress is obtained at the heel of the bond wire which is exactly where the main bond wire failure modes occur. The 1D thermal model allows checking quickly the temperature distribution. We also measured the displacement of the bonding wires in different experimental configurations: single, or two parallel wires with or without active chip connection. We pointed out relevant Z-displacement that can lead to fatigue failure mode.

5 References

[1] M. Ciappa, "*Selected failure mechanisms of modern power modules",* Microelectronics Reliability (2002) 42, pp 653–667, PII : S00 2 6-2 7 14 (02) 0 00 4 2-2.

[2] A. Castellazzi *et al*. "*Electro-thermal model of a high-voltage IGBT module for realistic simulation of power converters*", IEEE Solid State Device Research Conf., 2007. 11-13 Sept. 2007, pp 155 – 158, Munich, ISSN : 1930-8876,

[3] H. A Schafft, "*Faillure analysis of wire bonds*", Reliability Physics Symposium, 11th Annual Issue, April 1973, pp: 98 – 104, NV, USA, ISSN: 0735-0791

[4] S. Ramminger, *et al* "*Crack Mechanism in wire bonding joints",* Microelectronics Reliability, 38 (1998) pp 1301-1305, PII: S0026-2714(98)00141-3.

[5] Scilab open source software, http://www.scilab.org/